Received xxx/xxxx; | Revised xxx/xxxx; | Accepted xxx/xxxx

DOI: xxx/xxxx

RESEARCH ARTICLE

Dynamics of a harvested cyanobacteria-fish model with modified Holling type IV functional response

Shengyu Huang[1,2] | Hengguo Yu[1,2] | Chuanjun Dai[2,3] | Zengling Ma[2,3] | Qi Wang[2,3] | Min Zhao*[2,3]

[1] School of Mathematics and Physics, Wenzhou University, Wenzhou, Zhejiang, 325035, CHINA

[2] Key Laboratory for Subtropical Oceans & Lakes Environment and Biological Resources Utilization Technology of Zhejiang, Wenzhou University, Wenzhou, Zhejiang, 325035, CHINA

[3] School of Life and Environmental Science, Wenzhou University, Wenzhou, Zhejiang, 325035, CHINA

Correspondence
*Min Zhao, Wenzhou, Zhejiang, 325035, China. Email: zmcn@tom.com

ABSTRACT

In this paper, considering the aggregation effect and Allee effect of cyanobacteria population and the harvesting of both cyanobacteria and fish by human beings, we put forward a new cyanobacteria-fish model with two harvesting terms and a modified Holling type IV functional response function. The main purpose of this paper is to further understand the influence of harvesting terms on the dynamic behavior of cyanobacteria-fish model. Critical conditions for the existence and stability of several interior equilibria are given. The economic equilibria and the maximum sustainable total yield problem are also studied. The model exhibits several bifurcations, such as transcritical bifurcation, saddle-node bifurcation, Hopf bifurcation and Bogdanov-Takens bifurcation. From the perspective of biology, we conclude that the harvesting terms can determine the survival mode of cyanobacteria and fish. Finally, concrete examples of our model are given through numerical simulation to verify and enrich the theoretical results.

KEYWORDS:
Cyanobacteria-fish model, Allee effect, Harvesting, Aggregation effect, Bifurcation

1 | INTRODUCTION

Cyanobacteria are the oldest photosynthesizers and have promoted the formation of biosphere on the earth. However, cyanobacteria increasingly become dominant among other phytoplankton with the concentrations of TP and TN increase in the eutrophication process of rivers and lakes. Compared with other beneficial phytoplankton, cyanobacteria bloom will produce various toxic secondary metabolites (for example, cyanotoxins)[1,2], which will further cause certain damage to the natural ecosystems and human health. Nevertheless, cyanobacteria can be regarded as a potential solar biorefinery and continuously provide biofuels and chemicals when used properly[3,4,5]. Harvesting cyanobacteria can greatly reduce TP, TN and other nutrients then effectively prevent the deterioration of water eutrophication. The harvested cyanobacteria can be processed into compound organic fertilizer, organic biogas fertilizer as well as biogas with energy value for power generation or deep comprehensive utilization. Thus, harvesting cyanobacteria artificially can kill two birds with one stone in the aquatic area where cyanobacteria blooms. Among the various methods to control cyanobacteria bloom, the biological method based on the predation relationship between fish and cyanobacteria populations is widely used for its effectiveness, harmlessness and economic benefits. In recent years, researchers have done a lot of research on controlling algae by fish and zooplankton[6,7]. And mathematical researchers usually use differential equation model to analyze the dynamic relationship between species, the predator-prey model has been widely studied by researchers[8,9,10] since it was put forward. On the other hand, the extensive demand of human for fish resources

has also prompted the cultivation and harvesting of fish in as many water ecosystems as possible. Considering the growth rates, biomasses and harvesting intensities of cyanobacteria and fish, a reasonable harvesting plan should be made by the managers of biological resource to maintain sustainable fish resources and low density of cyanobacteria population.

The harvesting term is a vital element in ecological models, since it has great significance to the development of species population and economic growth. The paper[11] found that there exists a bistable region of their model when a Michaelis-Menten harvesting term to the predator population was introduced, they also derived the threshold of harvesting efforts to achieve the maximum economic benefits under the premise of sustainable development. The paper[12] proposed a deterministic and stochastic fractional-order model of tri-trophic food chain with harvesting term, and concluded that the dynamic of the second predator can be controlled by the harvesting parameters. The paper[13] concluded that the harvesting term plays an important role in the dynamic properties of a predator-prey model with a nonlinear harvesting term and a square root type functional response for prey. More influence of harvesting on dynamic behaviors are investigated in papers[14,15,16,17].

Furthermore, there are many paper introduced prey refuge term to interaction mathematical model[18,19,20]. The paper[21] proposed a modified algae-fish model, then explained the influence on the dynamic properties of it caused by prey refuge and allee effect. Functional response function represents the biomass of prey captured by each predator unit time, and it is always used to express the dynamic of predator and prey. This function represents the flow of matter from the prey population to the predator population. A modified Holling type II functional response function was constructed in[21] according to the prey refuge. However, function $\frac{\alpha(x-m)y}{a+b(x-m)+(x-m)^2}$ is more practical, which is an improved Holling type IV and it can show such a phenomenon that the defense ability of cyanobacteria population is improved after aggregation.It is also worth mentioning that the harvesting terms of algae and fish by human beings are not considered in[21]. In this paper, we study the following cyanobacteria-fish model with two harvesting terms:

$$\begin{cases} \frac{dx}{dt} = r_1 x\left(1-\frac{x}{k}\right)\left(\frac{x}{n}-1\right) - \frac{\alpha(x-m)y}{a+b(x-m)+(x-m)^2} - q_1\gamma E x, \\ \frac{dy}{dt} = \beta\frac{\alpha(x-m)y}{a+b(x-m)+(x-m)^2} - d_1 y - q_2 E y, \end{cases} \tag{1.1}$$

where E is the harvesting effort of fish, γ is the proportional coefficient of harvesting effort between fish and cyanobacteria, and $q_i (i = 1, 2)$ represent the catchability coefficients of cyanobactiria and fish respectively. The biological significance of other parameters in model (1.1) is consistent with that in the paper[21]. For the convenience of discussion, we do the following parameter substitutions to reduce the number of parameters:

$$\tau = \alpha t,\ r = \frac{r_1}{\alpha},\ d = \frac{d_1}{\alpha},\ e_1 = \frac{q_1\gamma E}{\alpha},\ e_2 = \frac{q_2 E}{\alpha},$$

retanining t to denote τ then model (1.1) can be expressed as:

$$\begin{cases} \frac{dx}{dt} = rx\left(1-\frac{x}{k}\right)\left(\frac{x}{n}-1\right) - \frac{(x-m)y}{a+b(x-m)+(x-m)^2} - e_1 x \triangleq g^1(x,y), \\ \frac{dy}{dt} = \beta\frac{(x-m)y}{a+b(x-m)+(x-m)^2} - dy - e_2 y \triangleq g^2(x,y). \end{cases} \tag{1.2}$$

The rest of present paper is organized as follows: In Section 2, we give the critical conditions for the existence and stability of each equilibria. The economic equilibrium and the MSTY problem for model (1.2) are studied in Section 3. In Section 4, we discuss the local bifurcations of model (1.2), such as transcritical bifurcation, saddle-node bifurcation, Hopf bifurcation and Bogdanov-Takens bifurcation. With the help of numerical simulation, the dynamic behaviors of model (1.2) are studied when bifurcation occurs in Section 5. Finally, the paper ends with brief concluding remarks in Section 6.

2 | ANALYSIS OF EQUILIBRIA

In this section, we will discuss the critical conditions for the existence and stability of potential equilibria in model (1.2).

It is obvious that the trivial equilibrium $E_0(0,0)$ of model (1.2) is always exist, and there exists a predator-free equilibrium $(x_1, 0)$ $[res.\ (x_2, 0)]$ when $\Delta_1 \geq 0$ and $x_1 \geq m$ $[res.\ x_2 \geq m]$, where

$$x_1 = \frac{kr + nr - \sqrt{\Delta_1}}{2r},\ x_2 = \frac{kr + nr + \sqrt{\Delta_1}}{2r},\ \Delta_1 = r^2(k-n)^2 - 4re_1 nk.$$

Otherwise, model (1.2) will exist two interior equilibria $\left(x_1^*, y_1^*\right)$ and $\left(x_2^*, y_2^*\right)$ when $\Delta_2 \geq 0$, x_1^* and x_2^* are the zeros of the function $f(x)$, where

$$f(x) = -\left(d+e_2\right)(x-m)^2 + \left[\beta - \left(d+e_2\right)b\right](x-m) - a\left(d+e_2\right),$$

and the expression of the two interior equilibria can be written as:

$$x_1^* = m - \frac{b}{2} + \frac{\beta - \sqrt{\Delta_2}}{2\left(d+e_2\right)}, \quad x_2^* = m - \frac{b}{2} + \frac{\beta + \sqrt{\Delta_2}}{2\left(d+e_2\right)},$$

where

$$\Delta_2 = \left(bd + be_2 - \beta\right)^2 - 4a\left(d+e_2\right)^2,$$

corresponding, the expression of y_i^* $(i = 1, 2)$ can be expressed as:

$$y_i^* = \frac{\left[a + b\left(x_i^* - m\right) + \left(x_i^* - m\right)^2\right]\left[rx_i^*\left(1 - \frac{x_i^*}{k}\right)\left(\frac{x_i^*}{n} - 1\right) - e_1 x_i^*\right]}{x_i^* - m}.$$

It is worth mentioning that $y_i^* > 0$ satisfy the biological significance when $x_1 < x_1^* \leq x_2^* < x_2$.

The interior equilibrium $E_1^*\left(x_1^*, y_1^*\right)$ $\left[res.\ E_2^*\left(x_2^*, y_2^*\right)\right]$ exists under the biological significances when (1), (2) and (3)[$res.$ (4)] of the following conditions are satisfied:

(1). $\beta > b\left(d+e_2\right)$,

(2). $\Delta_1 > 0$, $\Delta_2 > 0$,

(3). $k + n + b - 2m - \frac{\sqrt{\Delta_1}}{r} < \frac{\beta - \sqrt{\Delta_2}}{d+e_2} < k + n + b - 2m + \frac{\sqrt{\Delta_1}}{r}$,

(4). $k + n + b - 2m - \frac{\sqrt{\Delta_1}}{r} < \frac{\beta + \sqrt{\Delta_2}}{d+e_2} < k + n + b - 2m + \frac{\sqrt{\Delta_1}}{r}$.

By model (1.2), the Jacobian matrix at $E(x, y)$ can be expressed as:

$$J_{E(x,y)} = \begin{bmatrix} a_{11}(x,y) & a_{12}(x) \\ a_{21}(x,y) & a_{22}(x) \end{bmatrix},$$

where

$$\begin{aligned}
a_{11}(x,y) &= -\frac{3r}{nk}x^2 + 2r\left(\frac{1}{n} + \frac{1}{k}\right)x - r + \frac{y\left(m^2 - 2mx + x^2 - a\right)}{\left[(x-m)^2 + b(x-m) + a\right]^2} - e_1, \\
a_{12}(x) &= -\frac{x-m}{(x-m)^2 + b(x-m) + a}, \\
a_{21}(x,y) &= -\frac{\beta y\left(m^2 - 2mx + x^2 - a\right)}{\left[(x-m)^2 + b(x-m) + a\right]^2}, \\
a_{22}(x) &= \frac{\beta(x-m)}{(x-m)^2 + b(x-m) + a} - d - e_2.
\end{aligned}$$

Based on the above analysis, we have the following theorems about the stability of the equilibria from the viewpoint of mathematics.

Theorem 1. Trivial extinction equilibrium $E_0(0,0)$ always exists and is a stable equilibrium.

Proof. The value of m must be equal to zero when $x = 0$ according to our previous assumptions, therefore the Jacobian matrix of E_0 can be written as:

$$J_{E_0(0,0)} = \begin{bmatrix} -r - e_1 & 0 \\ 0 & -d - e_2 \end{bmatrix},$$

it is obvious that matrix $J_{E_0(0,0)}$ has two negative characteristic roots $\lambda_1 = -r - e_1$ and $\lambda_2 = -d - e_2$. Therefore E_0 is stable according to the Routh-Hurwitz criterion. □

Theorem 2. The predator-free equilibrium $E_1\left(x_1, 0\right)$ is always unstable whenever it exists. E_1 is an unstable node or focus when the following three conditions are satisfied:

(1). $\Delta_1 > 0$,

(2). $\Delta_2 > 0$,

(3). $x_1 \in [m,k] \cap \left[x_1^*, x_2^*\right]$,
otherwise E_1 is a saddle under the following three conditions:
(4). $\Delta_1 > 0$,
(5). $x_1 \in [m,k]$,
(6). $\Delta_2 < 0 \vee x_1 \notin \left[x_1^*, x_2^*\right]$.

Proof. We know that x_1 is one of the roots of the equation $g^1(x,0) = 0$ according to the previous definition. It can be easily obtained that $a_{11}\left(x_1,0\right) = \left.\frac{dg^1(x,0)}{dx}\right|_{x=x_1} > 0$ for $0 < x_1 < x_2$ based on the properties of the cubics function $g^1(x,0)$. Since $a_{21}\left(x_1,0\right) = 0$, then $a_{11}\left(x_1,0\right)$ is one of the characteristic root of the Jacobian matrix $J_{E_1(x_1,0)}$ and the another root is $a_{22}\left(x_1,0\right)$. Only when the two conditions (2) and (3) are satisfied, $a_{22}\left(x_1,0\right) > 0$, which means both the two characteristic roots of $J_{E_1(x_1,0)}$ are positive, then E_1 is an unstable node or focus. Otherwise, $a_{22}\left(x_1,0\right) < 0$ when the conditions (5) and (6) are satisfied, then the equilibrium E_1 is a saddle since the two roots have opposite signs. □

Theorem 3. The other predator-free equilibrium $E_2\left(x_2,0\right)$ is a saddle when the following three conditions are satisfied:
(1). $\Delta_1 > 0$,
(2). $\Delta_2 > 0$,
(3). $x_2 \in [m,k] \cap \left[x_1^*, x_2^*\right]$,
otherwise it is a locally asymptotically stable node or focus under the following three conditions:
(4). $\Delta_1 > 0$,
(5). $x_2 \in [m,k]$,
(6). $\Delta_2 < 0 \vee x_2 \notin \left[x_1^*, x_2^*\right]$.

Proof. Obviously, x_2 is also a root of equation $g^1(x,0) = 0$, and we can obtain $a_{11}\left(x_2,0\right) = \left.\frac{dg^1(x,0)}{dx}\right|_{x=x_2} < 0$ through the similiar analysis. The element $a_{11}\left(x_2,0\right)$ is one of the characteristic roots of the Jacobian matrix $J_{E_2(x_2,0)}$ since $a_{21}\left(x_2,0\right) = 0$, and the other root is $a_{22}\left(x_2,0\right)$. The inequation $a_{22}\left(x_2,0\right) > 0$ will hold if and only if the conditions (2) and (3) are satisfied, in which case the Jacobian matrix $J_{E_2(x_2,0)}$ has two characteristic roots have opposite signs then E_2 is a saddle. Otherwise, both the two roots are negative under the conditions (4)-(6), then E_2 is a stable node or focus. □

Theorem 4. The interior equilibrium $E_1^*\left(x_1^*, y_1^*\right)$ is a saddle when it exists and $x_1^* > m + \sqrt{a}$. As for $x_1^* < m + \sqrt{a}$, E_1^* is a locally asymptotically stable equilibrium when $a_{11}\left(x_1^*, y_1^*\right) < 0$, while E_1^* is an unstable node or focus when $a_{11}\left(x_1^*, y_1^*\right) > 0$. The other interior equilibrium $E_2^*\left(x_2^*, y_2^*\right)$ is a saddle whenever it exists.

Proof. The Jacobian matrix of model (1.2) evaluated at the equilibrium E_i^* $(i = 1,2)$ can be written as:

$$J_{E_i^*(x_i^*,y_i^*)} = \begin{bmatrix} -\frac{3r}{nk}x_i^{*2} + 2r\left(\frac{1}{n}+\frac{1}{k}\right)x_i^* - r + \frac{y_i^*\left(m^2-2mx_i^*+x_i^{*2}-a\right)}{\left[\left(x_i^*-m\right)^2+b\left(x_i^*-m\right)+a\right]^2} - e_1 & -\frac{d+e_2}{\beta} \\ -\beta\frac{y_i^*\left(m^2-2mx_i^*+x_i^{*2}-a\right)}{\left[\left(x_i^*-m\right)^2+b\left(x_i^*-m\right)+a\right]^2} & 0 \end{bmatrix},$$

then the trace and the determinant of the Jacobian matrix can be written as:

$$Tr\left(J_{E_i^*}\right) = a_{11}\left(x_i^*, y_i^*\right), \quad Det\left(J_{E_i^*}\right) = -\frac{y_i^*\left(m^2 - 2mx_i^* + x_i^{*2} - a\right)\left(d + e_2\right)}{\left[\left(x_i^* - m\right)^2 + b\left(x_i^* - m\right) + a\right]^2}.$$

The sign of $Tr\left(J_{E_i^*}\right)$ cannot be directly obtained since the expression is too complicated, while the sign for $Det\left(J_{E_i^*}\right)$ is determined by the relationship between the values of x_i^* and $m + \sqrt{a}$. It can be easily obtained that $Det\left(J_{E_1^*}\right) > 0$ when $x_1^* < m + \sqrt{a}$ and $Det\left(J_{E_1^*}\right) < 0$ when $x_1^* > m + \sqrt{a}$. Furthermore, the Jacobian matrix has two characteristic roots with opposite signs and E_1^* is a saddle as $x_1^* > m + \sqrt{a}$. As for $x_1^* < m + \sqrt{a}$ is satisfied, the Jacobian matrix has two negative characteristic roots and E_1^* is a locally asymptotically stable equilibrium when $a_{11}\left(x_1^*, y_1^*\right) < 0$, but the Jacobian matrix has two positive characteristic roots and E_1^* is an unstable node or focus when $a_{11}\left(x_1^*, y_1^*\right) > 0$. However, it can be easily judged that the sign of $Det\left(J_{E_2^*}\right)$ is negative under the necessary condition for the existence of E_2^*: $\beta > b\left(d + e_2\right)$. Thus, E_2^* is always a saddle whenever it exists. □

3 | ANALYSIS OF HARVESTING

In this section, we will investigate the existence of economic equilibriua and discuss the MSTY problem in model (1.2).

3.1 | Economic equilibrium

The economic equilibrium can be obtained by the definition of $TC = TR$, where TC represents the cost for harvesting and TR refers to the full economic return on the obtained through harvesting. It is of great significance to study the existence of economic equilibrium since the total profit is directly determined by the relationship between TC and TR. Let c_1 and c_2 represent the cost of unit effort e_1 and e_2, respectively. Let p_1 represents the sum of the direct economic value generated by the comprehensive utilization of cyanobacteria per unit and the indirect economic value generated by the environmental quality improvement brought by harvesting cyanobacteria per unit. p_2 represents the economic benifit of unit population of fish. Then we have the following theorem.

Theorem 5. Model (1.2) has a non-trivial economic equilibrium when harvesting cyanobacteria and fish is profitable and the following condition is satisfied.

$$\frac{rc_1p_2\left(kp_1-c_1\right)\left(c_1-np_1\right)}{knc_2p_1^3} > \frac{c_2p_1\left(c_1-mp_1\right)}{p_2\left[ap_1^2+bp_1\left(c_1-mp_1\right)+\left(c_1-mp_1\right)^2\right]} > \frac{d}{\beta}.$$

Proof. The possible economic equilibria are determined by the following equations:

$$\begin{cases} rx\left(1-\frac{x}{k}\right)\left(\frac{x}{n}-1\right)-\frac{(x-m)y}{a+b(x-m)+(x-m)^2}-e_1x=0, \\ \beta\frac{(x-m)y}{a+b(x-m)+(x-m)^2}-dy-e_2y=0, \\ S=\left(p_1x-c_1\right)e_1+\left(p_2y-c_2\right)e_2=0. \end{cases}$$

From the above equations, we can obtain

$$\begin{aligned} &x_\infty=\frac{c_1}{p_1},\ \ y_\infty=\frac{c_2}{p_2}, \\ &e_{1\infty}=r\left(1-\frac{x_\infty}{k}\right)\left(\frac{x_\infty}{n}-1\right)-\frac{\left(x_\infty-m\right)y_\infty}{\left[a+b\left(x_\infty-m\right)+\left(x_\infty-m\right)^2\right]x_\infty}, \\ &e_{2\infty}=\beta\frac{x_\infty-m}{a+b\left(x_\infty-m\right)+\left(x_\infty-m\right)^2}-d, \end{aligned}$$

and the efforts are positive when the above condition is satisfied, therefore there exists a non-trival econimic equilibrium $\left(x_\infty, y_\infty, e_{1\infty}, e_{2\infty}\right)$ in model (1.2). □

3.2 | Maximum sustainable total yield

For a multi-species model with several harvesting terms, we always tend to gain the maximum sustainable total yield (MSTY)[22,23], which is the maximum biomass of total harvested populations varies with harvesting efforts under the premise of ensuring that all species can survive continuously. It is necessary to ensure the persistence of the populations, however interior equilibrium E_2^* is a saddle whenever it exists, thus we analysis the existence of MSTY in model (1.2) at interior equilibrium E_1^*. The expression of the total yield function at E_1^* can be written as follows:

$$Y\left(e_1,e_2\right)=e_1x_1^*+e_2y_2^*=e_1x_1^*+\frac{e_2\left[a+b\left(x_1^*-m\right)+\left(x_1^*-m\right)^2\right]\left[rx_1^*\left(1-\frac{x_1^*}{k}\right)\left(\frac{x_1^*}{n}-1\right)-e_1x_1^*\right]}{x_1^*-m}.$$

The two efforts of harvesting e_1^* and e_2^* should satisfy $\partial Y\left(e_1^*,e_2^*\right)/\partial e_1=\partial Y\left(e_1^*,e_2^*\right)/\partial e_2=0$ or $Y\left(e_1^*,e_2^*\right)$ is the nondifferentiable point of function $Y\left(e_1,e_2\right)$ when the MSTY exists. It is obvious that $Y\left(e_1,e_2\right)$ is a linear function with respect to e_1, which means $\partial^2Y\left(e_1,e_2\right)/\partial e_1^2=0$. Therefore, we can not directively tell the exsitence of the MSTY through the Hessian

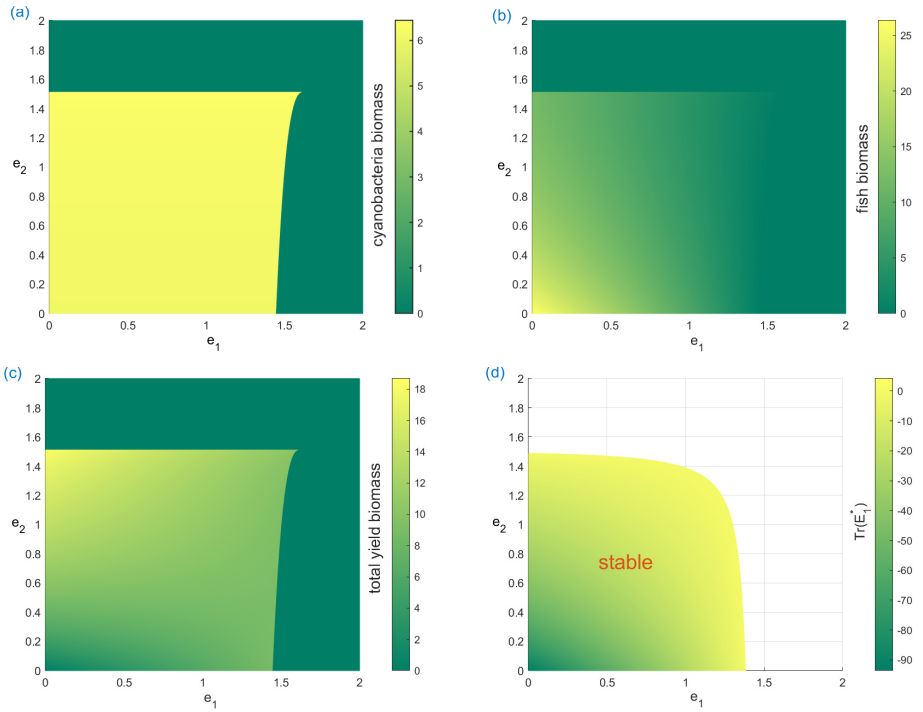

FIGURE 1 (a) The biomass of prey at E_1^* with varying harvesting efforts. (b) The biomass of predator at E_1^* with varying harvesting efforts. (c) The total yield biomass of predator and prey at E_1^* with varying harvesting efforts. (d) The stable area of interior equilibrium E_1^*, in this area $Det\left(E_1^*\right)$ is always positive.

matrix. We give a numerical simulation since the expression of the yield function is too complex to analysis, and the values are taken as:

$$k = 100,\ n = 3,\ m = 6,\ \beta = 3,\ r = 1.5,\ d = 1,\ a = 0.2,\ b = 0.3.$$

The biomasses of prey and predator at equilibrium E_1^* and the total yield varie with harvesting efforts e_1 and e_2 are shown as Fig.1. It can be seen from Fig.1 (a) that the influences of e_1 and e_2 on the biomass of cyanobacteria at E_1^* are very small firstly, but cyanobacteria will be extinct when $e_2 > 1.5117$ or fish is extinct. With the increase of the harvesting efforts e_1 and e_2, the biomass of fish at E_1^* gradually decreases and tends to become extinct, as is shown in Fig.1 (b). From fig.1 (c), we can get that the total yield biomass reaches the maximum at the nondifferentiable point $(0, 1.5117, 18.7706)$. However, the interior equilibrium E_1^* is unstable at this point according to Fig.1 (d), which implies that there is no MSTY in model (1.2). We always harvest both cyanobacteria and fish at different efforts in real life. Moreover, we study the MSTY problem of model (1.2) when the two harvesting efforts are in a certain proportion. Assuming that the harvesting efforts $e_1 = \lambda e_2$, then the total yield function can be expressed as:

$$H(e) = Y\left(e, \frac{e}{\lambda}\right).$$

Let's take different value of λ and analyze it by numerical simulation. It can be seen from Fig. 2 that with the increase of harvesting effort e, the fish population decreases sharply and tends to be extinct at E_1^*, while the cyanobacteria population keep steady, and the total yield biomass increases firstly and then changes smoothly, the interior equilibrium E_1^* disappears with the extinction of fish finally. In addition, the solid line in Fig. 2 indicates stability and the dashed line indicates instability based on Theorem 4. The total yield function reaches its sustainable maximum at $H(1.0389) = 10.8641$ when $\lambda = 1$, and at $H(1.2701) = 9.2723$ when $\lambda = 2$.

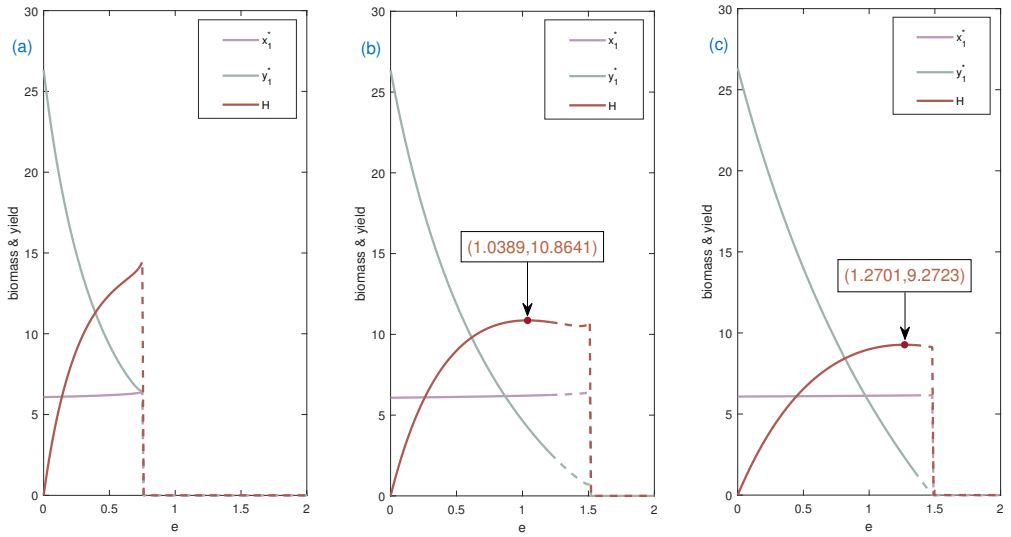

FIGURE 2 The population densities and total yield biomass $H(e)$ with varying harvesting efforts at E_1^*. (a) $\lambda = 0.5$. (b) $\lambda = 1$. (c) $\lambda = 2$.

4 | LOCAL BIFURCATION

In this section, we will discuss the local bifurcation in model (1.2) theoretically. We take the aggregation parameter m and harvesting efforts e_1 and e_2 as the bifurcation parameters, transcritical bifurcation, saddle-node bifurcation and Hopf bifurcation with codimension 1 and Bogdanov-Takens bifurcation with codimension 2 are analyzed successively.

4.1 | Transcritical bifurcation

Transcritical bifurcation always occurs at the boundary equilibria, since the equiulibrium E_1 is unstable whenever it exists, therefore transcritical bifurcation will only happen at E_2. The transcritical bifurcations are caused by the collisions of interior equilibria E_1^* or E_2^* with E_2, choosing aggregration parameter m as the bifurcation parameter, then we can obtain the expressions of the critical value correspondingly

$$m_1 = \frac{b+k+n}{2} + \frac{\sqrt{\Delta_1}}{2r} + \frac{\sqrt{\Delta_2}-\beta}{2\left(d+e_2\right)}, \quad m_2 = \frac{b+k+n}{2} + \frac{\sqrt{\Delta_1}}{2r} - \frac{\sqrt{\Delta_2}+\beta}{2\left(d+e_2\right)}.$$

Then, if m_1 or m_2 are in the set $[0,k]$, the predator-free equilibrium E_2 will translate its stability as the value of parameter m passes through m_1 or m_2.

Theorem 6. The model (1.2) will undergo a transcritical bifurcation at the equilibrium E_2 when $m = m_1 \in [0,k]$ or $m = m_2 \in [0,k]$.

Proof. When $m = m_1 \in [0,k]$, the elements of Jacobian matrix $J_{(E_2;m_1)}$ are

$$a_{11}\left(x_2,0\right), \quad a_{12}\left(x_2\right)|_{m=m_1}, \quad a_{21}\left(x_2,0\right) = a_{22}\left(x_2\right)|_{m=m_1} = 0,$$

letting V and W are eigenvectors of zero eigenvalues of $J_{(E_2;m_1)}$ and $J^T_{(E_2;m_1)}$ respectively. Without loss of generality, we can take

$$V = \begin{pmatrix} v_1 \\ v_2 \end{pmatrix} = \begin{pmatrix} -a_{12}\left(x_2\right)\Big|_{m=m_1} \\ a_{11}\left(x_2,0\right) \end{pmatrix}, \quad W = \begin{pmatrix} w_1 \\ w_2 \end{pmatrix} = \begin{pmatrix} 0 \\ 1 \end{pmatrix},$$

then

$$W^T F_m\left(E_2;m_1\right)=\begin{pmatrix}0&1\end{pmatrix}\left.\begin{pmatrix}-\frac{y\left[(x-m)^2-a\right]}{\left[a+b(x-m)+(x-m)^2\right]^2}\\ \frac{\beta y\left[(x-m)^2-a\right]}{\left[a+b(x-m)+(x-m)^2\right]^2}\end{pmatrix}\right|_{\left(E_2;m_1\right)}=\begin{pmatrix}0&1\end{pmatrix}\begin{pmatrix}0\\0\end{pmatrix}=0,$$

$$W^T\left[DF_m\left(E_2;m_1\right)V\right]=\begin{pmatrix}0&1\end{pmatrix}\left.\begin{pmatrix}0&-\frac{(x-m)^2-a}{\left[a+b(x-m)+(x-m)^2\right]^2}\\0&\frac{\beta\left[(x-m)^2-a\right]}{\left[a+b(x-m)+(x-m)^2\right]^2}\end{pmatrix}\right|_{\left(E_2;m_1\right)}\begin{pmatrix}-a_{12}\left(x_2\right)\Big|_{m=m_1}\\a_{11}\left(x_2,0\right)\end{pmatrix}$$

$$=\left.\frac{a_{11}(x,y)\,\beta\left[(x-m)^2-a\right]}{\left[a+b(x-m)+(x-m)^2\right]^2}\right|_{\left(E_2;m_1\right)}$$

$$W^T\left[D^2F_m(E_2;m_1)(V,V)\right]=\begin{pmatrix}w_1&w_2\end{pmatrix}\left.\begin{pmatrix}g^1_{xx}&g^1_{xy}&g^1_{yx}&g^1_{yy}\\g^2_{xx}&g^2_{xy}&g^2_{yx}&g^2_{yy}\end{pmatrix}\right|_{\left(E_2;m_1\right)}\begin{pmatrix}v_1v_1\\v_1v_2\\v_2v_1\\v_2v_2\end{pmatrix}$$

$$=\frac{2\beta\left[a-\left(x_2-m_1\right)^2\right]\left[3rx_2^2-2r(k+n)x_2+kn\left(r+e_1\right)\right]\left(m_1-x_2\right)}{nk\left[a+b\left(x_2-m_1\right)+\left(x_2-m_1\right)^2\right]^3},$$

Since the conditions for the establishment of equations

$$W^T\left[DF_m(E_2;m_1)V\right]=0,\ \ W^T\left[D^2F_m(E_2;m_1)(V,V)\right]=0$$

are very harsh, therefore the above two equations will not hold within a wide range of parameters, which means that the model (1.2) undergoes a transcritical bifurcation at equilibrium E_1 within these parameter ranges according to the *Sotomayor's Theorem*.

The proof process of the theorem when $m=m_2\in[0,k]$ is omitted since it is similar to the above. □

4.2 | Saddle-node bifurcation

On the basis of the previous analysis of the existence of the equilibria and some right conditions, it is obvious that the predator-free equilibria E_1 and E_2 will overlap as an equilibrium $E_{sn}\left(x_{sn},y_{sn}\right)$ when $\Delta_1=0$, and the interior equilibria will also overlap as an equilibrium $E^*_{sn}\left(x^*_{sn},y^*_{sn}\right)$ when $\Delta_2=0$. These dynamic phenomenos are caused by two saddle-node bifurcations, then we have the following two Theorems.

Theorem 7. Model (1.2) will undergo a saddle-node bifurcation at the equilibrium $E_{sn}\left(x_{sn},y_{sn}\right)$ with respect to e_1 as the bifurcation parameter when the parameters satisfy the two conditions:

(1). $2m<k+n$,

(2). $e_1=e_{1sn}=\frac{r(k-n)^2}{4nk}$.

Proof. Now we verify the transversality condition for the occurrence of saddle-node bifurcation at $e_1=e_{1sn}$ using the *Sotomayor's Theorem*. The equilibrium E_{sn} exists under the conditions (1) and (2) according to the previous analysis, the Jacobian matrix at E_{sn} can be written as

$$J_{E_{sn}}=\begin{pmatrix}0&-\frac{x_{sn}-m}{\left(x_{sn}-m\right)^2+b\left(x_{sn}-m\right)+a}\\0&\frac{\beta\left(x_{sn}-m\right)}{\left(x_{sn}-m\right)^2+b\left(x_{sn}-m\right)+a}-d-e_2\end{pmatrix},$$

where $x_{sn}=\frac{k+n}{2}$, corresponding $y_{sn}=0$. It is obvious that $Det\left(J_{E_{sn}}\right)=0$, such that zero is one of the eigenvalue of $J_{E_{sn}}$. Letting V and W represent eigenvertors corresponding to the eigenvalue zero for the matrices $J_{E_{sn}}$ and $J^T_{E_{sn}}$. Assuming that the

equilibrium E_{sn} do not coincide with E_1^* or E_2^*, such that $f\left(x_{sn}\right) \neq 0$, then without loss of generality, we can take

$$V = \begin{pmatrix} v_1 \\ v_2 \end{pmatrix} = \begin{pmatrix} 1 \\ 0 \end{pmatrix}, \quad W = \begin{pmatrix} w_1 \\ w_2 \end{pmatrix} = \begin{pmatrix} 1 \\ \frac{x_{sn}-m}{f\left(x_{sn}\right)} \end{pmatrix},$$

such that

$$W^T F_{e_1}\left(E_{sn}; e_{1sn}\right) = \begin{pmatrix} w_1 & w_2 \end{pmatrix} \begin{pmatrix} -x_{sn} \\ 0 \end{pmatrix} = -x_{sn} \neq 0,$$

$$W^T \left[D^2 F_{e_1}\left(E_{sn}; e_{1sn}\right)(V,V)\right] = \begin{pmatrix} w_1 & w_2 \end{pmatrix} \begin{pmatrix} g_{xx}^1 & g_{xy}^1 & g_{yx}^1 & g_{yy}^1 \\ g_{xx}^2 & g_{xy}^2 & g_{yx}^2 & g_{yy}^2 \end{pmatrix}\Bigg|_{\left(E_{sn}; e_{1sn}\right)} \begin{pmatrix} v_1v_1 \\ v_1v_2 \\ v_2v_1 \\ v_2v_2 \end{pmatrix}$$

$$= -\frac{r(k+n)}{kn} \neq 0$$

Hence the eigenvectors V and W satisfy the transversality conditions, such that model (1.2) occurs a saddle-node bifurcation at E_{sn} when $e_1 = e_{1sn}$.. □

Theorem 8. Model (1.2) will undergo a saddle-node bifurcation at the equilibrium $E_{sn}^*\left(x_{sn}^*, y_{sn}^*\right)$ with respect to e_2 as the bifurcation parameter when the parameters satisfy the three conditions:

(1). $\beta > b\left(d + e_2\right)$,

(2). $e_2 = e_{2sn} = \frac{\beta}{2\sqrt{a}+b} - d > 0$,

(3). $\left(2mr + 2r\sqrt{a} - kr - nr\right)^2 < \Delta_1$.

Proof. Similiar to the proof process about the above theorem, we need to verify the transversality condition for the occurrence of saddle-node bifurcation at $e_2 = e_{2sn}$. The interior equilibrium $E_{sn}^*\left(x_{sn}^*, y_{sn}^*\right)$ exists under the above three conditions according to the previous analysis of equilibria, where

$$x_{sn}^* = m + \sqrt{a}, \quad y_{sn}^* = \left(2\sqrt{a} + b\right)\left[rx_{sn}^*\left(1 - \frac{x_{sn}^*}{k}\right)\left(\frac{x_{sn}^*}{n} - 1\right) - e_1 x_{sn}^*\right]$$

and the Jacobian matrix at E_{sn}^* can be written as

$$J_{E_{sn}^*} = \begin{pmatrix} a_{11}\left(x_{sn}^*, y_{sn}^*\right) & -\frac{1}{b+2\sqrt{a}} \\ 0 & 0 \end{pmatrix},$$

Letting V and W represent eigenvertors corresponding to the eigenvalue zero for the matrices $J_{E_{sn}^*}$ and $J_{E_{sn}^*}^{*T}$, and without loss of generality, we can take

$$V = \begin{pmatrix} v_1 \\ v_2 \end{pmatrix} = \begin{pmatrix} \frac{1}{b+2\sqrt{a}} \\ a_{11}\left(x_{sn}^*, y_{sn}^*\right) \end{pmatrix}, \quad W = \begin{pmatrix} w_1 \\ w_2 \end{pmatrix} = \begin{pmatrix} 0 \\ 1 \end{pmatrix},$$

hence

$$W^T F_{e_2}\left(E_{sn}^*; e_{2sn}\right) = \begin{pmatrix} w_1 & w_2 \end{pmatrix} \begin{pmatrix} 0 \\ -y_{sn}^* \end{pmatrix} = -y_{sn}^* \neq 0,$$

$$W^T \left[D^2 F_{e_2}\left(E_{sn}^*; e_{2sn}\right)(V,V)\right] = \begin{pmatrix} w_1 & w_2 \end{pmatrix} \begin{pmatrix} g_{xx}^1 & g_{xy}^1 & g_{yx}^1 & g_{yy}^1 \\ g_{xx}^2 & g_{xy}^2 & g_{yx}^2 & g_{yy}^2 \end{pmatrix}\Bigg|_{\left(E_{sn}^*; e_{2sn}\right)} \begin{pmatrix} v_1v_1 \\ v_1v_2 \\ v_2v_1 \\ v_2v_2 \end{pmatrix}$$

$$= -\frac{2\beta y_{sn}^*}{\sqrt{a}\left(b + 2\sqrt{a}\right)^4} \neq 0.$$

Therefor, the eigenvectors V and W satisfy the transversality conditions for the occurrence of saddle-node bifurcation at the interior equilibrium E_{sn}^* when $e_2 = e_{2sn}$. In addition, as the value of e_2 passes through e_{2sn}, there is an interior equilibrium in model (1.2) and then it becomes two. □

4.3 | Hopf bifurcation

In this subsection, we concentrate on the occurrence of Hopf bifurcation at the interior equilibrium E_1^* of model (1.2) based on the previous discussion about the stability of the interior equilibria.

In order to study Hopf bifurcation in model (1.2), we take harvesting effort e_1 as bifurcation parameter, and require that $e_1 = e_{1hp}$ is a positive root of $a_{11}\left(x_1^*, y_1^*\right) = 0$. The stability of the interior equilibrium E_1^* changes when e_1 passes through e_{1hp}, then we obtain the following theorem.

Theorem 9. Model (1.2) will undergo a Hopf bifurcation at the interior equilibrium $E_1^*\left(x_1^*, y_1^*\right)$ when $e_1 = e_{1hp}$ and the other parameters satisfy the following three conditions:

(1). $\Delta_1 > 0$,

(2). $\Delta_2 > 0$,

(3). $\max\left\{m, x_1\right\} < x_1^* < \min\left\{m + \sqrt{a}, x_2, k\right\}$.

Proof. It is easy to testify that the interior equilibrium E_1^* exists and $Det\left(J_{E_1^*}\right)|_{e_1=e_{1hp}} > 0$ is satisfied under the above three conditions. Since we have set $a_{11}\left(x_1^*, y_1^*\right)|_{e_1=e_{1hp}} = 0$, i.e. the trace of $J_{E_1^*}$ is zero, thus we only need to verify the transversality condition for Hopf bifurcation. It can be easily obtained that

$$\frac{d}{de_1}Tr\left(J_{E_1^*}\right)\Big|_{e_1=e_{1hp}} = \frac{-2x_1^{*3} + (5m-b)x_1^{*2} + 2m(b-2m)x_1^* + m\left(m^2 - bm + a\right)}{\left(x_1^* - m\right)^3 + b\left(x_1^* - m\right)^2 + a\left(x_1^* - m\right)}.$$

Since the condition for the establishment of the equation $\frac{d}{de_1}Tr\left(J_{E_1^*}\right)\Big|_{e_1=e_{1sn}} = 0$ is so harsh that the transversality condition for Hopf bifurcation is satisfied within a wide range of parameters.

In order to evaluate the stability of the interior equilibrium E_1^* after Hopf bifurcation, we calculate the first Lyapunov number l_1 at the equilibrium E_1^* of model (1.2). Firstly, translate E_1^* into the origin $(0,0)$, letting $x^* = x - x_1^*$ and $y^* = y - y_1^*$, then model (1.2) can be expressed as

$$\begin{cases} \dot{x^*} = \alpha_{10}x^* + \alpha_{01}y^* + \alpha_{20}x^{*2} + \alpha_{11}x^*y^* + \alpha_{02}y^{*2} + \alpha_{30}x^{*3} + \alpha_{21}x^{*2}y^* + \alpha_{12}x^*y^{*2} + \alpha_{03}y^{*3} + P_1, \\ \dot{y^*} = \beta_{10}x^* + \beta_{01}y^* + \beta_{20}x^{*2} + \beta_{11}x^*y^* + \beta_{02}y^{*2} + \beta_{30}x^{*3} + \beta_{21}x^{*2}y^* + \beta_{12}x^*y^{*2} + \beta_{03}y^{*3} + +P_2, \end{cases}$$

According to the previous content, we can obtain that $Tr\left(J_{E_1^*}\right) = \alpha_{10} + \beta_{01} = 0$ and $Det\left(J_{E_1^*}\right) = \alpha_{10}\beta_{02} - \alpha_{01}\beta_{10} > 0$, the other parameters α_{ij} and β_{ij} can be seen in the Appendix A. P_1 and P_2 are the remainder terms in Taylor series of $\dot{x^*}$ and $\dot{y^*}$. The first Lyapunov number l_1 can be expressed as follows according to the expression of it in paper[24].

$$l_1 = \frac{-3\pi}{2\sqrt{-\alpha_{01}^3\beta_{10}}}\left(\alpha_{11}\alpha_{20} - 3\alpha_{01}\alpha_{30} - \alpha_{01}\beta_{21}\right).$$

Furthermore, when $e_1 = e_{1sn}$, model (1.2) will undergo a supercritical Hopf bifurcation at the interior equilibrium E_1^* if $l_1 < 0$, but the Hopf bifurcation is subcritical if $l_1 > 0$. For the expression of l_1 is too cumbersome to determine the sign of it, we will give a numerical example in the next section to increase its reliability. □

4.4 | Bogdanov-Takens bifurcation

It is necessary for us to investigate the joint influence of e_1 and e_2 on model (1.2) since the harvesting efforts of cyanobacteria and fish are always not constant in real life. In this subsection, we select e_1 and e_2 as Bogdanov-Takens bifurcation parameters to study the influence on the dynamic behavior caused by the harvesting efforts theoretically.

Theorem 10. Model (1.2) will undergo a Bogdanov-Takens bifurcation at $\left(e_{1bt}, e_{2bt}\right)$ when e_1 and e_2 are chosen as the bifurcation parameters. And the two harvesting efforts e_{1bt} and e_{2bt} satisfy the following two conditions:

$$Det\left[J_{E_1^*}\right]|_{(e_{1bt},e_{2bt})}=0,\ \ Tr\left[J_{E_1^*}\right]|_{(e_{1bt},e_{2bt})}=0.$$

In order to analyze the dynamic behavior of model (1.2) within a small range of B-T point, we firstly calculate the local expressions of saddle-node bifurcation, Hopf bifurcation and homoclinic bifurcation through translating model (1.2) into a normal form.

For harvesting efforts, we introduce two small disturbance ξ_1 and ξ_2, i.e., substituting $e_1 = e_{1bt} + \xi_1$ and $e_1 = e_{2bt} + \xi_2$ in model (1.2), then follows:

$$\begin{cases} \frac{dx}{dt} = rx\left(1-\frac{x}{k}\right)\left(\frac{x}{n}-1\right) - \frac{(x-m)y}{a+b(x-m)+(x-m)^2} - \left(e_{1bt}+\xi_1\right)x, \\ \frac{dy}{dt} = \beta\frac{(x-m)y}{a+b(x-m)+(x-m)^2} - dy - \left(e_{2bt}+\xi_2\right)y. \end{cases} \tag{4.1}$$

After taking the variable substitutions $u_1 = x - x_1^*$ and $u_2 = y - y_1^*$, the equilibrium E_1^* comes to the origin, and model (4.1) becomes:

$$\begin{cases} \frac{du_1}{dt} = p_{00}\left(\xi_1,\xi_2\right) + p_{10}\left(\xi_1,\xi_2\right)u_1 + \alpha_{01}u_2 + \alpha_{20}u_1^2 + \alpha_{11}u_1u_2 + \alpha_{02}u_2^2, \\ \frac{du_2}{dt} = q_{00}\left(\xi_1,\xi_2\right) + \beta_{10}u_1 + q_{01}\left(\xi_1,\xi_2\right)u_2 + \beta_{20}u_1^2 + \beta_{11}u_1u_2 + \beta_{02}u_2^2 + P_3, \end{cases} \tag{4.2}$$

where $p_{00}\left(\xi_1,\xi_2\right) = -\xi_1 x_1^*$, $p_{10}\left(\xi_1,\xi_2\right) = -\xi_1$, $q_{00}\left(\xi_1,\xi_2\right) = -\xi_2 y_1^*$, $q_{01}\left(\xi_1,\xi_2\right) = -\xi_2$, the other parameters α_{ij} and β_{ij} are consistent with the previous, and P_3 is the remainder term in Taylor series of $\frac{du_2}{dt}$ in model (4.2).

Then we substitute the variables in model (4.2) near the origin as follows:

$$v_1 = u_1,\ \ v_2 = p_{00}\left(\xi_1,\xi_2\right) + p_{10}\left(\xi_1,\xi_2\right)u_1 + \alpha_{01}u_2 + \alpha_{20}u_1^2 + \alpha_{11}u_1u_2,$$

under the substitutions, model (4.2) becomes

$$\begin{cases} \frac{dv_1}{dt} = v_2, \\ \frac{dv_2}{dt} = c_{00}\left(\xi_1,\xi_2\right) + c_{10}\left(\xi_1,\xi_2\right)v_1 + c_{01}\left(\xi_1,\xi_2\right)v_2 + c_{20}\left(\xi_1,\xi_2\right)v_1^2 + c_{11}\left(\xi_1,\xi_2\right)v_1v_2 + c_{02}\left(\xi_1,\xi_2\right)v_2^2 + P_4, \end{cases} \tag{4.3}$$

the expressions of c_{ij} can be seen in the Appendix B and P_4 is the remainder term in Taylor series of $\frac{dv_2}{dt}$ in model (4.3).

A new time variable τ is introduced to further transform model (4.3) into the normal form, such that $\left(1 - c_{02}\left(\xi\right)v_1\right)d\tau = dt$. We rewrite t to denote τ for simplicity. Then, under the change of $w_1 = v_1$, $w_2 = v_2\left(1 - c_{02}v_1\right)$, model (4.3) becomes

$$\begin{cases} \frac{dw_1}{dt} = w_2, \\ \frac{dw_2}{dt} = \theta_{00}\left(\xi_1,\xi_2\right) + \theta_{10}\left(\xi_1,\xi_2\right)w_1 + \theta_{01}\left(\xi_1,\xi_2\right)w_2 + \theta_{20}\left(\xi_1,\xi_2\right)w_1^2 + \theta_{11}\left(\xi_1,\xi_2\right)w_1w_2 + P_5, \end{cases} \tag{4.4}$$

where

$$\begin{aligned} &\theta_{00}\left(\xi_1,\xi_2\right) = c_{00}\left(\xi_1,\xi_2\right),\ \ \theta_{10}\left(\xi_1,\xi_2\right) = c_{10}\left(\xi_1,\xi_2\right) - 2c_{00}\left(\xi_1,\xi_2\right)c_{02}\left(\xi_1,\xi_2\right),\ \ \theta_{01}\left(\xi_1,\xi_2\right) = c_{01}\left(\xi_1,\xi_2\right), \\ &\theta_{20}\left(\xi_1,\xi_2\right) = c_{20}\left(\xi_1,\xi_2\right) - 2c_{10}\left(\xi_1,\xi_2\right)c_{02}\left(\xi_1,\xi_2\right) + c_{00}\left(\xi_1,\xi_2\right)c_{02}^2\left(\xi_1,\xi_2\right), \\ &\theta_{11}\left(\xi_1,\xi_2\right) = c_{11}\left(\xi_1,\xi_2\right) - 2c_{01}\left(\xi_1,\xi_2\right)c_{02}\left(\xi_1,\xi_2\right), \end{aligned}$$

and P_5 is the remainder term in Taylor series of $\frac{dw_2}{dt}$ in model (4.4).

let $z_1 = w_1 + \frac{\theta_{10}(\xi_1,\xi_2)}{2\theta_{20}(\xi_1,\xi_2)}$, $z_2 = w_2$, then model (4.4) has the following new form:

$$\begin{cases} \frac{dz_1}{dt} = z_2, \\ \frac{dz_2}{dt} = \sigma_{00}\left(\xi_1,\xi_2\right) + \sigma_{01}\left(\xi_1,\xi_2\right)z_2 + \sigma_{20}\left(\xi_1,\xi_2\right)z_1^2 + \sigma_{11}\left(\xi_1,\xi_2\right)z_1z_2 + P_6, \end{cases} \tag{4.5}$$

where

$$\begin{aligned} &\sigma_{00}\left(\xi_1,\xi_2\right) = \theta_{00}\left(\xi_1,\xi_2\right) - \frac{\theta_{10}^2\left(\xi_1,\xi_2\right)}{4\theta_{20}\left(\xi_1,\xi_2\right)},\ \ \sigma_{01}\left(\xi_1,\xi_2\right) = \theta_{01}\left(\xi_1,\xi_2\right) - \frac{\theta_{10}\left(\xi_1,\xi_2\right)\theta_{11}\left(\xi_1,\xi_2\right)}{2\theta_{20}\left(\xi_1,\xi_2\right)}, \\ &\sigma_{20}\left(\xi_1,\xi_2\right) = \theta_{20}\left(\xi_1,\xi_2\right),\ \ \sigma_{11}\left(\xi_1,\xi_2\right) = \theta_{11}\left(\xi_1,\xi_2\right), \end{aligned}$$

and P_6 is the remainder term in Taylor series of $\frac{dz_2}{dt}$ in model (4.5).

In order to simplify the coefficient of term $\sigma_{20}\left(\xi_1,\xi_2\right)z_1^2$ in model (4.5), we let

$$s_1 = z_1,\ \ s_2 = \frac{z_2}{\sqrt{\left|\sigma_{20}\left(\xi_1,\xi_2\right)\right|}},\ \ \tau = t\sqrt{\left|\sigma_{20}\left(\xi_1,\xi_2\right)\right|},$$

rewriting t to denote τ, then model (4.5) has a new form:

$$\begin{cases} \frac{ds_1}{dt} = s_2, \\ \frac{ds_2}{dt} = \gamma_{00}\left(\xi_1,\xi_2\right) + \gamma_{01}\left(\xi_1,\xi_2\right) s_2 + \gamma_{20}\left(\xi_1,\xi_2\right) s_1^2 + \gamma_{11}\left(\xi_1,\xi_2\right) s_1 s_2 + P_7, \end{cases} \tag{4.6}$$

where

$$\gamma_{00}\left(\xi_1,\xi_2\right) = \frac{\sigma_{00}\left(\xi_1,\xi_2\right)}{\left|\sigma_{20}\left(\xi_1,\xi_2\right)\right|},\ \ \gamma_{01}\left(\xi_1,\xi_2\right) = \frac{\sigma_{01}\left(\xi_1,\xi_2\right)}{\sqrt{\left|\sigma_{20}\left(\xi_1,\xi_2\right)\right|}},$$
$$\gamma_{20}\left(\xi_1,\xi_2\right) = \frac{\sigma_{20}\left(\xi_1,\xi_2\right)}{\left|\sigma_{20}\left(\xi_1,\xi_2\right)\right|},\ \ \gamma_{11}\left(\xi_1,\xi_2\right) = \frac{\sigma_{11}\left(\xi_1,\xi_2\right)}{\sqrt{\left|\sigma_{20}\left(\xi_1,\xi_2\right)\right|}},$$

and P_7 is the remainder term in Taylor series of $\frac{ds_2}{dt}$ in model (4.6).

Supposing $\sigma_{11} \neq 0$, then $\gamma_{11} \neq 0$. Further setting

$$x = \frac{\sigma_{20}\left(\xi_1,\xi_2\right)}{\left|\sigma_{20}\left(\xi_1,\xi_2\right)\right|}\gamma_{11}^2\left(\xi_1,\xi_2\right) s_1,\ \ y = \gamma_{11}^3\left(\xi_1,\xi_2\right) s_2,\ \ \tau = \frac{\sigma_{20}\left(\xi_1,\xi_2\right)}{\left|\sigma_{20}\left(\xi_1,\xi_2\right)\right| \gamma_{11}\left(\xi_1,\xi_2\right)} t,$$

rewriting t to denote τ, we obtain the normal form of model (4.1) at B-T point

$$\begin{cases} \frac{dx}{dt} = y, \\ \frac{dy}{dt} = \varpi_{00}\left(\xi_1,\xi_2\right) + \varpi_{01}\left(\xi_1,\xi_2\right) y + x^2 + xy + P_8, \end{cases} \tag{4.7}$$

where

$$\varpi_{00}\left(\xi_1,\xi_2\right) = \frac{\sigma_{20}\left(\xi_1,\xi_2\right)}{\left|\sigma_{20}\left(\xi_1,\xi_2\right)\right|}\gamma_{00}\left(\xi_1,\xi_2\right)\gamma_{11}^4\left(\xi_1,\xi_2\right),\ \ \varpi_{01}\left(\xi_1,\xi_2\right) = \frac{\sigma_{20}\left(\xi_1,\xi_2\right)}{\left|\sigma_{20}\left(\xi_1,\xi_2\right)\right|}\gamma_{01}\left(\xi_1,\xi_2\right)\gamma_{11}\left(\xi_1,\xi_2\right),$$

and P_8 is the remainder term in Taylor series of $\frac{d\varpi_2}{dt}$ in model (4.7).

Based on the results of[25], model (1.2) undergoes a Bogdanov-Takens bifurcation when $\left(e_1,e_2\right) = \left(e_{1bt},e_{2bt}\right)$ and $\left(\xi_1,\xi_2\right)$ is in a small domain of the origin. We obtain the local expressions of the following three bifurcation curves.

(1). The curve of saddle-node bifurcation:
$SN = \left\{\left(\xi_1,\xi_2\right) : \varpi_{00}\left(\xi_1,\xi_2\right) = 0, \varpi_{01}\left(\xi_1,\xi_2\right) \neq 0\right\}$;

(2). The curve of Hopf bifurcation:
$Hp = \left\{\left(\xi_1,\xi_2\right) : \varpi_{01}\left(\xi_1,\xi_2\right) = \frac{\sigma_{20}\left(\xi_1,\xi_2\right)}{\left|\sigma_{20}\left(\xi_1,\xi_2\right)\right|}\sqrt{-\varpi_{00}\left(\xi_1,\xi_2\right)}, \varpi_{00}\left(\xi_1,\xi_2\right) < 0\right\}$;

(3). The curve of homoclinic bifurcation:
$HL = \left\{\left(\xi_1,\xi_2\right) : \varpi_{01}\left(\xi_1,\xi_2\right) = \frac{5\sigma_{20}\left(\xi_1,\xi_2\right)}{7\left|\sigma_{20}\left(\xi_1,\xi_2\right)\right|}\sqrt{-\varpi_{00}\left(\xi_1,\xi_2\right)}, \varpi_{00}\left(\xi_1,\xi_2\right) < 0\right\}$.

5 | NUMERICAL SIMULATION

Although we have obtained some theoretical results of model (1.2) in the previous sections, it is not easy to get intuitional knowing about the dynamic behaviors of the model since some expressions in the theory analysis are truly complicated. Thus, we perform some precise numerical simulations to further research the model and investigate the dynamic behavior of it in this section. Throughout the numerical simulations, we consider a set of hypothetical values of parameters according to their biological signification in model (1.2):

$$k = 50,\ n = 3,\ m = 30,\ \beta = 0.6,\ r = 1.5,\ d = 1,\ a = 0.02,\ b = 0.1.$$

Under this parameters, we can obtain the Hopf bifurcation curves of model (1.2) as Fig.3 (a). Then, we fix the harvesting effort $e_1 = 3.194748196$ additionally, and let the another effort e_2 vary within in a small range. We can get a bifurcation diagram of model (1.2) as Fig.3 (b). There take place a Hopf bifurcation and saddle-node bifurcation when $e_2 = 0.5672232479$ and $e_2 = 0.5672232498$ respectively. The solid line in Fig. 3 (b) indicates stability and the dashed line indicates instability. Fig.4 reveals the detailed evolution process of Hopf bifurcation.

The Bogdanov-Takens bifurcation parameters are calculated as $e_{1bt} = 3.194748196$ and $e_{2bt} = 0.5672232498$ on the premise of the above parameters. The biomasses of cyanobacteria at interior equilibria E_1^* and E_2^* with varying harvesting efforts are shown in Fig.5 (a). Although it is not obvious, the curves lying on the curved surface of x_1^* in Fig.5 (a) are saddle-node, Hopf and homoclinic bifurcation curves respectively. The projections of these curves on $e_1 - e_2$ plane within a small range of $\left(e_{1bt}, e_{2bt}\right)$ can be clearly seen in Fig.5 (b). These bifurcation curves divide the left area of Bogdanov-Takens bifurcation point in the $\xi_1 - \xi_2$ plane into four blocks and named then as I, II, III and IV. Go through the SN curve top-down, there generates an interior equilibrium and then evolves into two. There appears or disappears a periodic oscillation solution with the transform of the stability of interior equilibrium E_1^* when the parameters locate on the Hp curve. Along the HL curve, the limit cycle becomes homoclinic orbit after connecting with E_2^* and then disappears. Next, we will investigate the dynamic properties and corresponding biological significance within the four regions and on the curves through analyzing the phase diagrams at the six locations (a)-(f) in Fig.5 (b).

At location (a): $(-0.02, 0.0000000002)$, there exist trivial equilibrium E_0(black dot in Fig.6 (a)) and predator-free equilibria E_1(red dot in Fig.6 (a)) and E_2(blue dot in Fig.6 (a)). But only the equilibrium E_2 is meaningful in the perspective of biology, since the biomass of cyanobacteria must be greater than the aggregation amount according to the definition of model (1.2), and the parameter of aggregation is m=30 at this time. The predator-free equilibrium E_2 is a globally stable node here in the biological sense, which means the population of fish will become extinct eventually and the cyanobacteria will remain at the corresponding density of E_2. The time series evolution and phase portrait of the model at location (a) can be seen as Fig.6 (a).

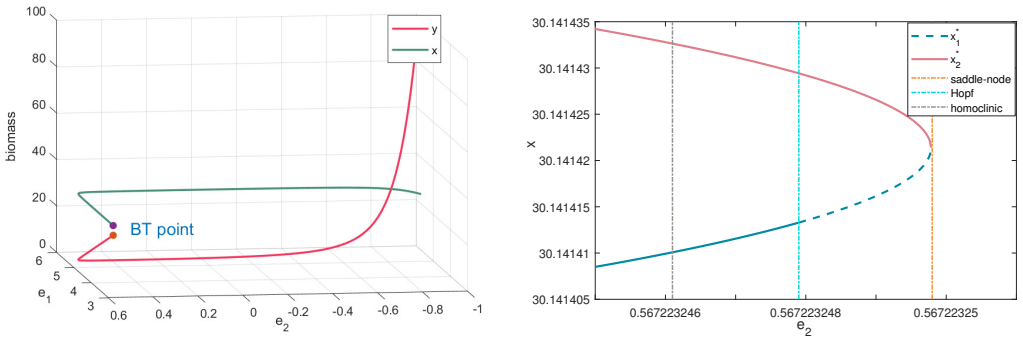

FIGURE 3 (a). Hopf bifurcation curves of model (1.2) under the previous parameters. (b). Bifurcation diagram of model (1.2) under the previous parameters and $e_1 = 3.174748196$.

The location (b): $(-0.02, 0)$, is on the SN curve. There exists a saddle-node equilibrium E_{sn}^*(blue dot in Fig.6 (b)), which will evolve into two interior equilibria E_1^* and E_2^* as the two parameters enter region II from region I. In addition, the trivial equilibrium and the two predator-free equilibria are also exist at this time. Similar to location (a), only E_{sn}^* and E_2 are meaningful from the biological point of view. Fish will eventually become extinct and the density of cyanobacteria will remains at the corresponding density of E_2 due to the instability of E_{sn}^*. The time series evolution and phase portrait near interior equilibrium E_{sn}^* are presented in Fig.6 (b).

There arise two interior equilibria E_1^*(red dot in Fig.6 (c)) and E_2^*(blue dot in Fig.6 (c)) from E_{sn}^* at location (c): $(-0.02, -0.0000000016)$, E_1^* and E_2^* are unstable focus and unstable saddle respectively. The remaining equilibrium at this position has similar dynamic behavior as at position (b). Fig.6 (c) presents the time series evolution and phase portrait around the interior equilibria. With the evolution of time, the final destiny of the two populations is consistent with the position (b), that is, the fish is extinct and the population density of cyanobacteria tends to be stable.

The Hp curve has a significant influence on the dynamic behavior of model (1.2). When we move position (c) through Hp curve to (d): $(-0.02, -0.0000000029)$, a Hopf bifurcation occurs in the model. A semistable limit cycle(red cycle in Fig.6 (d)) arises around the interior equilibrium E_1^*, the value of first Lyapunov number l_1 is -3149722.203π at this time, which indicates that the interior equilibrium E_1^* becomes stable after a supercritical Hopf bifurcation. With the evolution of time, the trajectory within a small range outside the limit cycle tends to the limit cycle, while the trajectory of the inside is far away from it and converges to the interior equilibrium E_1^*. Therefore, when the initial population density of fish and cyanobacteria falls in different areas on the $\xi_1 - \xi_2$ plane, three different biological phenomena may occur. The first destiny is the same as the results in positions

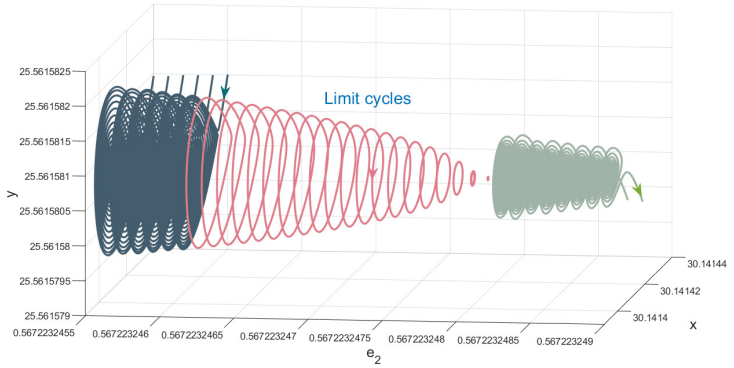

FIGURE 4 The progresses of homoclinic bifurcation and Hopf bifurcation in model (1.2) with the previous parameters and $e_1 = 3.174748196$.

(a)-(c), which means the fish will extinct and the population density of cyanobacteria keeps at a stable state. The second result is that fish and cyanobacteria coexist, and their population densities maintain periodically oscillation with time, but this periodic oscillation coexistence mode is unstable, which will convert to the third coexistence mode at stable focus E_1^* under a small disturbance from outside.

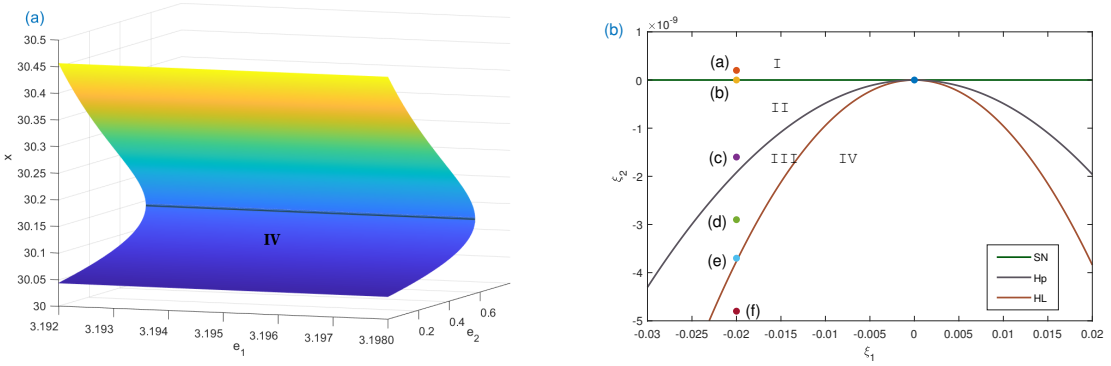

FIGURE 5 (a) The biomasses of prey at E_1^* and E_2^* with varying harvesting efforts. (b) Three bifurcation curves of model (1.2), which is another manifestation of lines between x_1^* and x_2^* in (a).

The limit cycle becomes larger gradually, and then connects with saddle equilibrium E_2^* to form a homoclinic orbit(red cycle in Fig.6 (e)) in the process of moving down from position (d) to position (e): $(-0.02, -0.0000000037)$ on curve HL. The remaining equilibrium at this position has similar dynamic behavior as at position (d). The two species of fish and cyanobacteria will eventually coexist at the interior equilibrium E_1^* when the initial density of the two populations falls within the homoclinic orbit. While on the homoclinic orbit or outside, the fish will eventually become extinct and the population density of cyanobacteria tends to the predator-free equilibrium of E_2 and then remains stable.

When the parameters are located at position (f): $(-0.02, -0.0000000048)$ in region IV, the homoclinic orbit disappears, where E_1^* is a stable focus and E_2^* is a saddle, the properties of other equilibria are consistent with those at position (e). The two populations will coexist at the interior equilibrium E_1^*, or the fish will extinct and the cyanobacteria population finally remains stable depending on the initial population density. Therefore, an ideal ecological pattern can be guided to form through controlling the initial population density artificially.

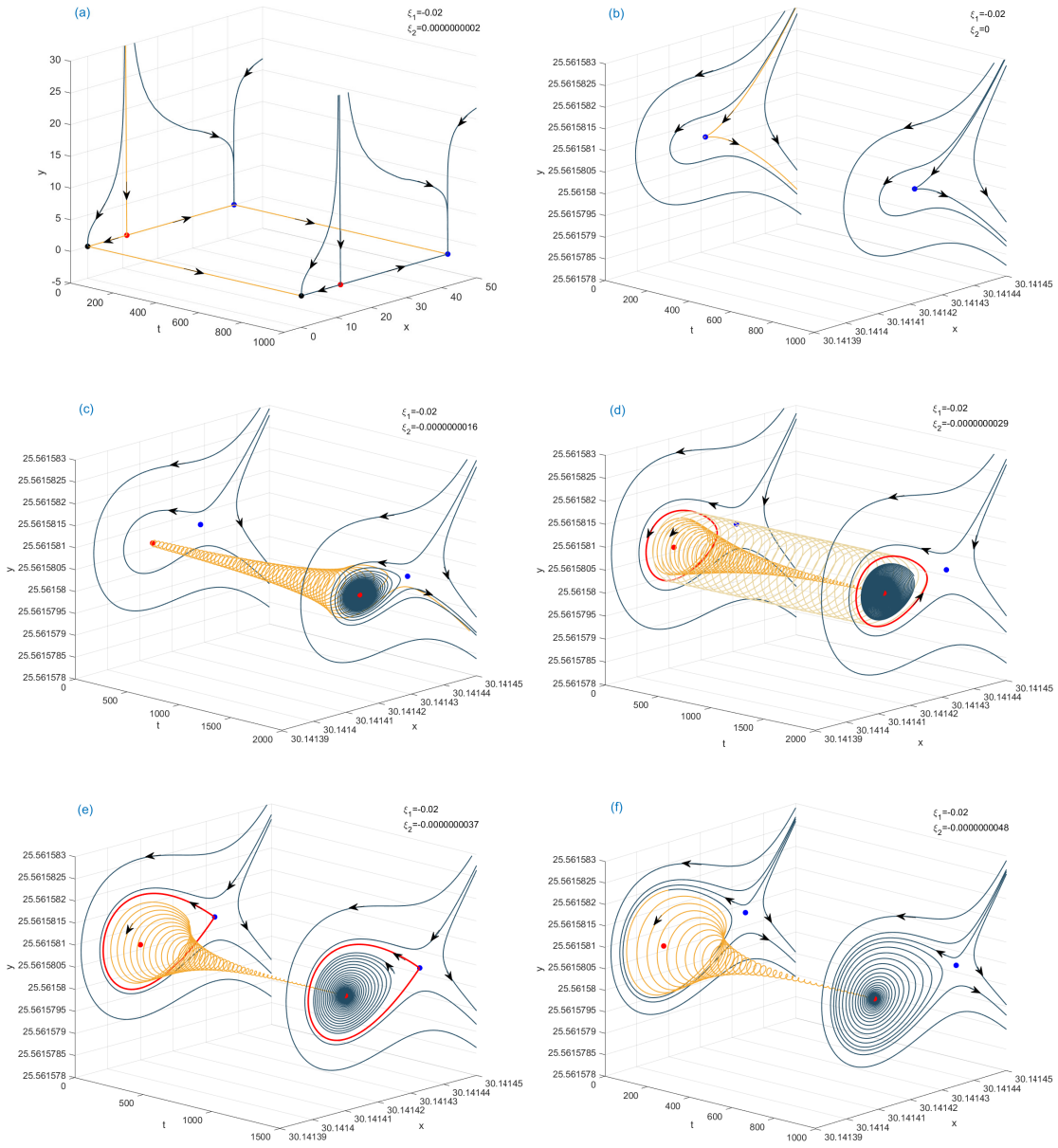

FIGURE 6 Phase portraits and time series evolution of model (1.2) with varying ξ_1 and ξ_2 around Bogdanov-Takens point $(0, 0)$.

6 | CONCLUSIONS

This paper proposed a cyanobacteria-fish model with two harvesting terms and modified Holling type IV functional response function on the basis of predator-prey model. The critical conditions are analyzed firstly, to make certain the existence and stability of potential equilibria in model (1.2), which is the preparatory work for the later theoretical analysis. We concluded that there is an economic equilibrium in model (1.2), and MSTY exists at the interior equilibrium E_1^* under certain parameters through analyzing the harvesting efforts. This has an enlightening effect on the managers of water ecological resources. That is, on the premise of ensuring that cyanobacteria do not break out and fish do not become extinct, they can choose to obtain the maximum and stable total yield at MSTY point. Harvesting efforts e_1 and e_2 are chosen as our bifurcation parameters,

and the existence of saddle-node bifurcation and Hopf bifurcation with codimension 1 and Bogdanov-Takens bifurcation with codimension 2 in the model are analyzed. The theoretical conditions of their occurrence are given simultaneously.

In the section of simulation analysis, the analysis of bifurcation theory in model (1.2) are further enriched with concrete numerical examples and corresponding biological explanations. According to the phase portraits and time series evolution of the model when the parameters are taken in different regions on the bifurcation diagram, we obtained the dynamic behaviors and explained the corresponding biological significances. This provides an inspiration for the water ecological resources managers to formulate reasonable harvesting strategies. That is, they can promote the development of the two populations to reach their expected target, through controlling the initial population densities of cyanobacteria and fish and adopting harvesting efforts with corresponding intensity. It is also one of the important significances of our paper. In addition, formulating mature and practical harvesting strategies in the further research is necessary.

The influence of different harvesting terms on the dynamic behaviors of the model needs further consideration, and we will verify the reliability of the model through experiments in the follow-up work. Of course, in order to make our model reflect the real situation within a small range of error, we need to improve the model according to many factors. For example, after introducing other species, multi-preys or multi-predators model is constructed according to a series of survival relationships between them. We can also analyze the current model in more detail according to the age structure of the populations or considering the spatial diffusion behavior of the species.

ACKNOWLEDGEMENTS

This work was supported by the National Natural Science Foundation of China (Grants No. 61871293 and No. 61901303), the National Key Research and Development Program of China (Grant No. 2018YFE0103700).

CONFLICT OF INTEREST

The authors declare no potential conflict of interests.

References

1. Paerl HW, Otten TG. Harmful cyanobacterial blooms: causes, consequences, and controls. *Microb Ecol.* 2013;65(4):995—1010.

2. Serrà A, Philippe L, Perreault F, Garcia-Segura S. Photocatalytic treatment of natural waters. Reality or hype? The case of cyanotoxins remediation. *Water Res.* 2021;188:116543.

3. Włodarczyk A, Selão TT, Norling B, Nixon PJ. Newly discovered Synechococcus sp. PCC 11901 is a robust cyanobacterial strain for high biomass production. *Commun Biol.* 2020;215(3).

4. Shahid A, Usman M, Atta Z, et al. Impact of wastewater cultivation on pollutant removal, biomass production, metabolite biosynthesis, and carbon dioxide fixation of newly isolated cyanobacteria in a multiproduct biorefinery paradigm. *Bioresource Technol.* 2021;333:125194.

5. Chandrasekhar K, Raj T, Ramanaiah SV, et al. Algae biorefinery: A promising approach to promote microalgae industry and waste utilization. *J Biotechnol.* 2022;345:1-16.

6. Öğlü B, Bhele U, Järvalt A, et al. Is fish biomass controlled by abiotic or biotic factors? Results of long-term monitoring in a large eutrophic lake. *J Great Lakes Res.* 2020;46(4):881-890.

7. Shen RJ, Gu XH, Chen HH, Mao ZG, Zeng QF, Jeppesen E. Combining bivalve (Corbicula fluminea) and filter-feeding fish (Aristichthys nobilis) enhances the bioremediation effect of algae: An outdoor mesocosm study. *Sci Total Environ.* 2020;727:138692.

8. Arancibia-Ibarra C, Aguirre P, Flores J, Heijster PV. Bifurcation analysis of a predator-prey model with predator intraspecific interactions and ratio-dependent functional response. *Appl Math Comput.* 2021;402:126152.

9. Zou XL, Li QW, Lv JL. Stochastic bifurcations, a necessary and sufficient condition for a stochastic Beddington–DeAngelis predator–prey model. *Appl Math Lett.* 2021;117:107069.

10. Souna F, Lakmeche A, Djilali S. Spatiotemporal patterns in a diffusive predator-prey model with protection zone and predator harvesting. *Chaos Soliton Fract.* 2020;140:110180.

11. Ang TK, Safuan HM. Dynamical behaviors and optimal harvesting of an intraguild prey-predator fishery model with Michaelis-Menten type predator harvesting. *Biosystems.* 2021;202:104357.

12. M El-Shahed AM Al-Dububan. Deterministic and Stochastic Fractional-Order Hastings-Powell Food Chain Model. *CMC-Comput Mater Con.* 2022;70(2):2277–2296.

13. Mortuja MG, Chaube MK, Kumar S. Dynamic analysis of a predator-prey system with nonlinear prey harvesting and square root functional response. *Chaos Soliton Fract.* 2021;148:111071.

14. Bellier E, Sæther BE, Engen S. Sustainable strategies for harvesting predators and prey in a fluctuating environment. *Ecol Model.* 2021;440:109350.

15. Mezouaghi A, Djilali S, Bentout S, Biroud K. Bifurcation analysis of a diffusive predator-prey model with prey social behavior and predator harvesting. *Math Method Appl Sci.* 2022;45:718-731.

16. Al-Omari J, Gumah G, Al-Omari S. Dynamics of a harvested stage-structured predator–prey model with distributed maturation delay. *Math Method Appl Sci.* 2022;45(2):761-769.

17. Xie BF, Zhang ZC, Zhang N. Influence of the Fear Effect on a Holling Type II Prey-Predator System with a Michaelis-Menten Type Harvesting. *Int J Bifurcat Chaos.* 2021;31(14).

18. Molla H, Sarwardi S, Smith SR, Haque M. Dynamics of adding variable prey refuge and an Allee effect to a predator-prey model. *Alex Eng J.* 2022;61(6):4175-4188.

19. Barman D, Roy J, Alrabaiah H, Panja P, Mondal SP, Alam S. Impact of predator incited fear and prey refuge in a fractional order prey predator model. *Chaos Soliton Fract.* 2021;142.

20. Barman D, Roy J, Alrabaiah H, Panja P, Mondal SP, Alam S. Impact of predator incited fear and prey refuge in a fractional order prey predator model. *Chaos Soliton Fract.* 2021;142.

21. Huang SY, Yu HG, Dai CJ, Ma ZL, Wang Q, Zhao M. Dynamic analysis of a modified algae and fish model with aggregation and Allee effect. *Math Biosci Eng.* 2022;19(4):3673-3700.

22. Bapan G, Kar T, Legovic T. Sustainability of exploited ecologically interdependent species. *Popul Ecol.* 2014;56:527-537.

23. Paul P, Kar TK. Impacts of invasive species on the sustainable use of native exploited species. *Ecol Model.* 2016;340:106-115.

24. Shang ZC, Qiao YH, Duan LJ, Miao J. Bifurcation analysis in a predator–prey system with an increasing functional response and constant-yield prey harvesting. *Math Comput Simulat.* 2021;190:976-1002.

25. Huang JC, Ruan SG, Song J. Bifurcations in a predator–prey system of Leslie type with generalized Holling type III functional response. *J Differ Equations.* 2014;257(6):1721-1752.

How to cite this article:

APPENDIX

A .

$$\alpha_{10}=\alpha_{02}=\alpha_{12}=\alpha_{03}=\beta_{01}=\beta_{02}=\beta_{12}=\beta_{03}=0,$$

$$\alpha_{01}=-\frac{x_1^*-m}{\left(x_1^*-m\right)^2+b\left(x_1^*-m\right)+a},\quad \alpha_{11}=\frac{\left(x_1^*-m\right)^2-a}{\left[\left(x_1^*-m\right)^2+b\left(x_1^*-m\right)+a\right]^2},$$

$$\alpha_{20}=\frac{r}{kn}\left(n+k-3x_1^*\right)+\frac{y_1^*\left[-\left(x_1^*-m\right)^3+3a\left(x_1^*-m\right)+ab\right]}{\left[\left(x_1^*-m\right)^2+b\left(x_1^*-m\right)+a\right]^3},$$

$$\alpha_{30}=-\frac{3r}{kn}-\frac{y_1^*\left[7\left(x_1^*-m\right)^2+5b\left(x_1^*-m\right)+b^2-a\right]}{\left[\left(x_1^*-m\right)^2+b\left(x_1^*-m\right)+a\right]^3}+\frac{y_1^*\left[2\left(x_1^*-m\right)+b\right]^3}{\left[\left(x_1^*-m\right)^2+b\left(x_1^*-m\right)+a\right]^4},$$

$$\alpha_{21}=\frac{-\left(x_1^*-m\right)^3+3a\left(x_1^*-m\right)+ab}{\left[\left(x_1^*-m\right)^2+b\left(x_1^*-m\right)+a\right]^3},\quad \beta_{10}=-\frac{\beta y_1^*\left[\left(x_1^*-m\right)^2-a\right]}{\left[\left(x_1^*-m\right)^2+b\left(x_1^*-m\right)+a\right]^2},$$

$$\beta_{11}=-\frac{\beta\left[\left(x_1^*-m\right)^2-a\right]}{\left[\left(x_1^*-m\right)^2+b\left(x_1^*-m\right)+a\right]^2},\quad \beta_{20}=\frac{\beta y_1^*\left[\left(x_1^*-m\right)^3-3a\left(x_1^*-m\right)-ab\right]}{\left[\left(x_1^*-m\right)^2+b\left(x_1^*-m\right)+a\right]^3},$$

$$\beta_{30}=\frac{\beta y_1^*\left[7\left(x_1^*-m\right)^2+5b\left(x_1^*-m\right)+b^2-a\right]}{\left[\left(x_1^*-m\right)^2+b\left(x_1^*-m\right)+a\right]^3}-\frac{\beta y_1^*\left[2\left(x_1^*-m\right)+b\right]^3}{\left[\left(x_1^*-m\right)^2+b\left(x_1^*-m\right)+a\right]^4},$$

$$\beta_{21}=\frac{\beta\left[\left(x_1^*-m\right)^3-3a\left(x_1^*-m\right)-ab\right]}{\left[\left(x_1^*-m\right)^2+b\left(x_1^*-m\right)+a\right]^3}.$$

B .

$$c_{00}\left(\xi_1,\xi_2\right)=\alpha_{01}\left(\xi_1,\xi_2\right)q_{00}\left(\xi_1,\xi_2\right)-p_{00}\left(\xi_1,\xi_2\right)q_{01}\left(\xi_1,\xi_2\right),$$

$$c_{10}\left(\xi_1,\xi_2\right)=\alpha_{01}\left(\xi_1,\xi_2\right)\beta_{10}\left(\xi_1,\xi_2\right)+\alpha_{11}\left(\xi_1,\xi_2\right)q_{00}\left(\xi_1,\xi_2\right)-p_{00}\left(\xi_1,\xi_2\right)\beta_{11}\left(\xi_1,\xi_2\right)-p_{10}\left(\xi_1,\xi_2\right)q_{01}\left(\xi_1,\xi_2\right),$$

$$c_{01}\left(\xi_1,\xi_2\right)=p_{10}\left(\xi_1,\xi_2\right)+q_{01}\left(\xi_1,\xi_2\right)-\frac{\alpha_{11}\left(\xi_1,\xi_2\right)p_{00}\left(\xi_1,\xi_2\right)}{\alpha_{01}\left(\xi_1,\xi_2\right)},\quad c_{02}\left(\xi_1,\xi_2\right)=\frac{\alpha_{11}\left(\xi_1,\xi_2\right)}{\alpha_{01}\left(\xi_1,\xi_2\right)},$$

$$c_{20}\left(\xi_1,\xi_2\right)=\alpha_{01}\beta_{20}\left(\xi_1,\xi_2\right)+\alpha_{11}\beta_{10}\left(\xi_1,\xi_2\right)-\alpha_{20}\left(\xi_1,\xi_2\right)q_{01}\left(\xi_1,\xi_2\right)-p_{10}\left(\xi_1,\xi_2\right)\beta_{11}\left(\xi_1,\xi_2\right),$$

$$c_{11}\left(\xi_1,\xi_2\right)=\beta_{11}\left(\xi_1,\xi_2\right)+2\alpha_{20}\left(\xi_1,\xi_2\right)-\frac{\alpha_{11}\left(\xi_1,\xi_2\right)p_{10}\left(\xi_1,\xi_2\right)}{\alpha_{01}\left(\xi_1,\xi_2\right)}+\frac{\alpha_{11}^2\left(\xi_1,\xi_2\right)p_{00}\left(\xi_1,\xi_2\right)}{\alpha_{01}^2\left(\xi_1,\xi_2\right)},$$